PROCEEDINGS OF SCIENCE

First observation of the $\eta \to 4\mu$ decay with the CMS detector

Roberto Rossin for the CMS Collaboration[a,b,*]

[a] *Physics and Astronomy Department, Università di Padova, Via Marzolo 8, Padua, Italy*

[b] *Istituto Nazionale di Fisica Nucleare [INFN], Sezione di Padova, Via Marzolo 8, Padua, Italy*

E-mail: roberto.rossin@pd.infn.it

The first observation of the rare $\eta \to \mu^+\mu^-\mu^+\mu^-$ double-Dalitz decay is presented. The analysis is based on data collected by the CMS experiment at the CERN LHC operating at the centre-of-mass energy of $\sqrt{s} = 13\,\text{TeV}$. The data sample was collected with high-rate muon triggers for an integrated luminosity of $101\,\text{fb}^{-1}$.

The branching fraction of the $\eta \to 4\mu$ decay is measured relative to the $\eta \to 2\mu$ decay yielding a value of $\mathcal{B}(\eta \to \mu^+\mu^-\mu^+\mu^-) = [5.0 \pm 0.8(\text{stat}) \pm 0.7(\text{syst}) \pm 0.7(\mathcal{B}_{2\mu})] \times 10^{-9}$, in agreement with the Standard Model theoretical predictions.

The XVIth Quark Confinement and the Hadron Spectrum Conference (QCHSC24)
19-24 August, 2024
Cairns Convention Centre, Cairns, Queensland, Australia

*Speaker

 ISSN 1824-8039 . Published by SISSA Medialab.

PoS(QCHSC24)142

1. Introduction

The η and the η' mesons are neutral pseudoscalars composed of a mixing of light quark states. Their masses are $m_\eta = 547.9\,\mathrm{MeV/c^2}$ and $m_{\eta'} = 957.8\,\mathrm{MeV/c^2}$ [1]. The leptonic radiative decays of these particles can serve as precision tests for the standard model [2] and until recently the only observed leptonic radiative decays are $\eta \to \mu^+\mu^-$, $\eta \to e^+e^-e^+e^-$ and $\eta' \to e^+e^-e^+e^-$. The analysis reported here presents the first observation of the decay $\eta \to \mu^+\mu^-\mu^+\mu^-$ and the measurement of its branching fraction.

2. Detector and datasets

The data used in this analysis have been collected with the CMS detector in 2017 and 2018 at a centre-of-mass energy $\sqrt{s} = 13\,\mathrm{TeV}$ for a total integrated luminosity of $101\,\mathrm{fb^{-1}}$ [3, 4]. The CMS apparatus [5, 6] is a multipurpose detector, designed to trigger on [7–9] and identify electrons, muons, photons, and (charged and neutral) hadrons [10–12]. A global "particle-flow" (PF) algorithm [13] aims to reconstruct all individual particles in an event, combining information provided by the silicon inner tracker and by the crystal electromagnetic and brass-scintillator hadron calorimeters, operating inside a 3.8 T superconducting solenoid, with data from the gas-ionization muon detectors embedded in the flux-return yoke outside the solenoid. The reconstructed particles are used to build leptons, jets, and missing transverse momentum [14–16]. Events of interest are selected using a two-tiered trigger system. The first level (L1) uses information from the calorimeters and muon detectors to select events at a rate of around 100 kHz within a fixed latency of 4μs[7]. The second level, the high-level trigger (HLT), consists of a farm of processors running a version of the full event reconstruction software optimized for fast processing, and reduces the event rate to a few kHz before data storage [8, 9]. The HLT path used for the online selection is a double muon trigger that requires the presence of two muons with $p_T > 3\,\mathrm{GeV/c}$ and $|\eta| < 2.4$. In order to preserve high acceptance no di-muon invariant mass and no vertex displacement cuts are applied at trigger level. The data have been saved using a scouting technique [17] which consists in exchanging complete event information for higher trigger rates. Only the HLT objects have been saved allowing to collect more events. By reducing the event size by a factor of about 200 (the event size is $\sim 4 - 8kB$), very low-p_T muon triggers reaching close to $m_{\mu\mu} \geq 0.2\,\mathrm{GeV/c^2}$ can be used. The η meson is copiously produced in pp scattering at the LHC. Figure 1 shows a clearly visible peak in the $\mu\mu$ invariant mass spectrum in the scouting dataset, for a total of approximately 4.5M $\eta \to \mu\mu$. Using the its known branching fraction of $\mathcal{B}(\eta \to \mu\mu) = (5.8 \pm 0.8) \times 10^{-6}$ [1] the number of etas produced at CMS is estimated to be 10^{12} ηs. The theoretical prediction for the 4-muon branching fraction is $\mathcal{B}(\eta \to 4\mu) \sim 4 \times 10^{-9}$ [18], which implies that this decay mode should be in the reach of CMS.

3. Analysis strategy and event selection

The branching fraction $\mathcal{B}(\eta \to 4\mu)$, is related to the number of events $\eta \to 4\mu$ observed, $N_{4\mu}$:

$$N_{4\mu} = \int \mathcal{L}dt \cdot \sigma_{pp\to\eta+X} \cdot \mathcal{B}(\eta \to 4\mu) \cdot A_{4\mu}\,,$$

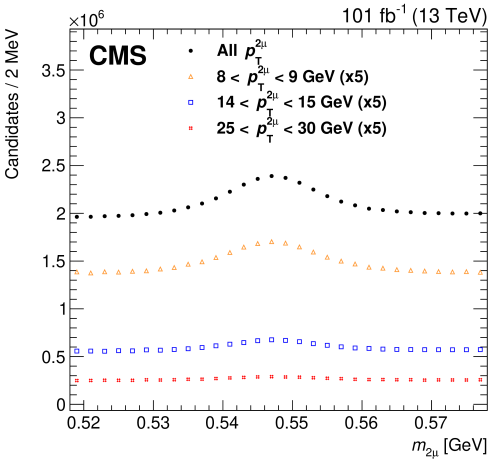

Figure 1: Distribution of $m_{\mu\mu}$ after the dimuon selection integrated in dimuon p_T and in three p_T ranges.[19]

where $\int \mathcal{L}dt$ is the integrated luminosity of the sample, $\sigma_{pp\to\eta+X}$ is the η inclusive production cross section at LHC (so $\int \mathcal{L}dt \cdot \sigma_{pp\to\eta+X}$ represents the total number of ηs produced in CMS) and $A_{4\mu}$ is the CMS total acceptance to $\eta \to 4\mu$ events defined as the product of the geometrical acceptance and the efficiency of the event selection (online and offline). The analysis strategy uses the $\eta \to 2\mu$ process as a reference channel, removing the need to measure directly the $\int \mathcal{L}dt \cdot \sigma_{pp\to\eta+X}$ and also reducing the uncertainty on the $A_{4\mu}$ acceptance. The events can be binned in p_T and $|y|$ of the reconstructed meson. For each bin (i, j) in $(p_T, |y|)$ it is possible to measure the quantities

$$N_{4\mu}^{i,j} = \int \mathcal{L}dt \cdot \sigma_{pp\to\eta+X} \cdot \mathcal{B}(\eta \to 4\mu) A_{4\mu}^{i,j},$$

and

$$N_{2\mu}^{i,j} = \int \mathcal{L}dt \cdot \sigma_{pp\to\eta+X} \cdot \mathcal{B}(\eta \to 2\mu) A_{2\mu}^{i,j}.$$

Taking the ratio bin-by-bin and summing over the bins:

$$N_{4\mu}^{i,j} = N_{2\mu}^{i,j} \cdot \frac{\mathcal{B}(\eta \to 4\mu)}{\mathcal{B}(\eta \to 2\mu)} \cdot \frac{A_{4\mu}^{i,j}}{A_{2\mu}^{i,j}} \quad \to \quad \mathcal{B}(\eta \to 4\mu) = \mathcal{B}(\eta \to 2\mu) \frac{N_{4\mu}}{\sum_{p_{T_i}, y_j} N_{2\mu}^{i,j} \frac{A_{4\mu}^{i,j}}{A_{2\mu}^{i,j}}}.$$

The $\mathcal{B}(\eta \to 2\mu)$ has been experimentally measured [1] with a precision of about 14%, the $N_{2\mu}^{i,j}$ can be measured for each bin in the reference channel, while the binned acceptances $A_{4\mu}^{i,j}$, $A_{2\mu}^{i,j}$ are estimated with Monte Carlo simulations (see section 4). The events collected by the di-muon scouting triggers are divided in two subsamples ($\eta \to 4\mu$ and $\eta \to 2\mu$) by requiring the presence of ≥ 2 or ≥ 4 muons in each event. The two-muon or four-muon invariant mass is computed for all combinations having a net charge of zero. The muons in the barrel region ($|\eta| < 1.2$) must have a $p_T > 3.5\,\text{GeV/c}$ (the lower part of the spectrum is polluted with fake muons). A Kalman vertex fitter is also applied to all pairs of muon candidates (for the four-muon selection this amounts to six pairs). By selecting events with high vertex probability and accepting only muon candidates associated with good vertexes more than 90% of the signal is retained (in the four-muon channel)

while about 85% of the background is rejected. Figure 2 shows the four-muon invariant mass distribution after the 4μ event selection fitted to a one-sided Crystal-Ball function for the signal and a threshold function, $\alpha(m_{4\mu} - 4m_{\mu})^{\beta}$, for the background ($\alpha$ and β are free parameters of the fit). The fit yiels $N_{4\mu} = 49.1 \pm 8.1$ signal events and 16.6 ± 0.6 background events (in the signal window). The parameters of the Crystal-Ball function have been fixed, except for the normalization, from the simulation. This amounts to a statistical significance in excess of 5 standard deviations.

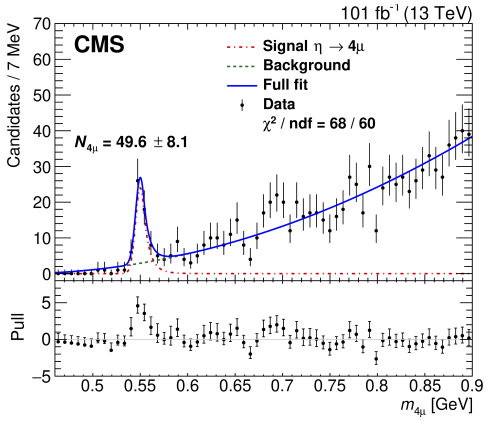

Figure 2: Measured four-muon invariant mass distribution, $m_{4\mu}$ fitted to a signal plus background shape.[19]

4. Signal simulation

The Monte Carlo simulation of the signal is generated with a custom workflow. The reason is that the predicted branching fraction is very small and the decay process is not present in the inclusive simulations. A standalone hadronic event generator called PLUTO [20], that contains the vector meson dominance model needed to simulate the rare η decays, has been adapted from the 4 electron channel to the 4 muon channel. The generator has been used as a particle gun, the decay products then boosted to the lab frame by sampling from uniform p_T and rapidity distributions in the $5 - 70\,\mathrm{GeV/c}$ and $|y| < 2.4$ ranges, respectively. The decay products are then embedded into complete CMS events, which also include the simulation of fragmentation, parton shower, and hadronization processes in the initial and final states with the PYTHIA 8.230 package [21], and simulation of the underlying event. The particle gun also adds the pileup on top of the four muons, resulting in a realistic simulation of how such a rare decay might appear in the CMS detector. The scouting triggering and reconstruction can then be applied to the MC simulation sample. With the described procedure two large samples of thousand decays per GeV/c of η meson p_T have been generated to measure the CMS acceptances to the $\eta \to 4\mu$ and $\eta \to 2\mu$ decays.

5. Acceptance measurements

The large samples of generated, triggered, reconstructed, and accepted signal events allow to measure the acceptances defined as the product of the trigger and reconstruction efficiencies for both the signal and the reference decays, combined with the requirement that both muons are compatible with beam spot production and the request of at least one vertex in the event. For the reference channel $\eta \to 2\mu$ the acceptance, $A^{ij}_{2\mu}$, is limited by the trigger efficiency (reaching a

plateau of about 70%). The turn on curve is shaped by the minimum p_T ($\sim 3.5\,\mathrm{GeV/c}$) required for a muon in the central region to reach the muon chambers. This is visible in Fig. 3 that shows the distribution of events as a function of the η p_T and split in two bins of rapidity (central and forward region). The same distributions for the 4-muon channel (Fig. 3) show a drop-off in the higher part of the spectrum, due to competing requirements on the muons to have sufficient p_T, and thus being produced by boosted ηs, and having sufficient angular separation to be reconstructed.

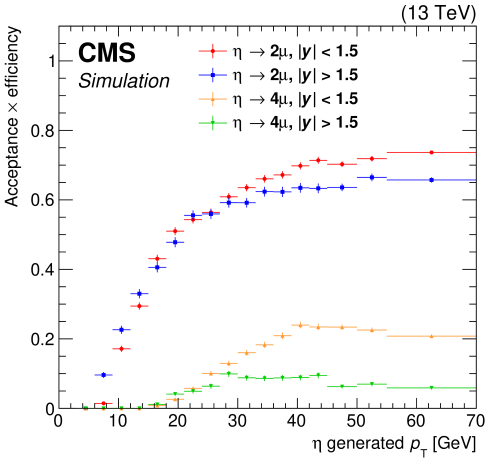

Figure 3: Total efficiencies for the 2-muon ($A^{ij}_{2\mu}$, red and blue points) and 4-muon ($A^{ij}_{4\mu}$, orange and green points) decay channels, as functions of the generated meson's p_T and y, evaluated with MC simulation.[19]

6. Backgrounds

The estimate of the signal yield relies on the assumption that there is no significant contribution of peaking backgrounds. Such kind of backgrounds consist of other η decay modes with $\pi \to \mu$ misidentification or $\gamma \to \mu\mu$ conversion. A comprehensive study of these modes has been carried out with toy Monte Carlo simulations. The decay chains are simulated via a series of two-body decays of the form $M \to m_1 m_2$. Figure 4 shows the predicted backgrounds contributions along with the signal peak. Backgrounds from η decay modes involving photons can arise when photons undergo conversion to muon pairs in the first layer of the inner tracker. These are modeled using GEANT4 [22] and the probability for this to happen is of the order of 10^{-15}, moreover there is an apparent upward mass shift of the photon (from 0 to $> 2m_\mu$) and the momentum transferred from the nucleus to the system turns this contribution into a non-peaking one. The only peaking background is $\eta \to \pi^+\pi^-\mu^+\mu^-$, where both pions are misidentified as muons. This mode has never been observed and the experimental upper limit on the branching fraction 1.6×10^{-4} [23] is much higher than the theoretical estimate $\mathcal{B} = 7.5 \times 10^{-9}$ [24]. The background estimate is based on the conservative assumption that the actual value is at its upper limit, still the loss of mass that results from the misidentification is significant and the peak shows up well below the signal.

The expected background in the signal region is then a non-resonant background. A further check of this prediction can be performed by estimating the four-muon p_T spectrum ($p_T^{4\mu}$) in the signal region mass window ($0.53 < m_{4\mu} < 0.57\,\mathrm{GeV/c^2}$) using the side-bands ($0.6 < m_{4\mu} <$

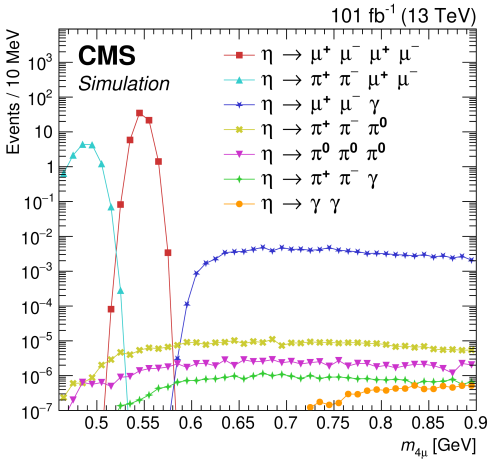

Figure 4: Predicted background contributions to the signal mass window, estimated with simplified MC simulations. The $\eta \to \mu^+\mu^-\mu^+\mu^-$ signal is displayed as a benchmark (red squares), followed by various other decay modes of the η meson. The curves are normalized to an integrated luminosity of 101 fb^{-1}.[19]

0.9 GeV/c^2). Figure 5 shows the predicted and observed $p_T^{4\mu}$ spectra for events in the signal mass window, a very good agreement between data and prediction is visible across the entire p_T range.

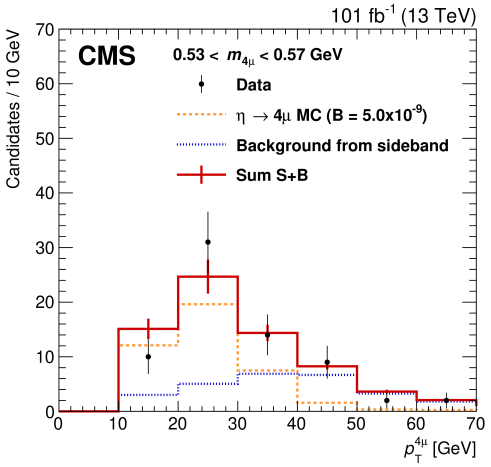

Figure 5: Predicted and observed $p_T^{4\mu}$ spectra for events in the signal mass window assuming the observed branching fraction (orange dashed line).[19]

7. Uncertainties

The measured quantity $\mathcal{B}(\eta \to 4\mu)$ is derived from the

$$\mathcal{B}_{4\mu} = \mathcal{B}_{2\mu} \frac{N_{4\mu}}{\sum_{pT_i, y_j} N_{2\mu}^{i,j} \frac{A_{4\mu}^{i,j}}{A_{2\mu}^{i,j}}}$$

and, because the measurement is done relative to the two-muon channel, a lot of the uncertainties cancel out. For example the luminosity, the PDF uncertainties and correction to simulations have no

impact, but a few uncertainties remain and need to be estimated. The uncertainty on the branching ratio of the reference channel is 14%[1], the statistical uncertainty on $N_{4\mu}$ is estimated from the fit shown in Fig. 2 and amounts to 16%. The statistical uncertainties on the $N_{2\mu}^{i,j}$ are instead negligible given the size of the $\eta \to 2\mu$ sample.

The remaining uncertainties are the systematic ones and are mainly related to the muon and trigger efficiencies evaluated by simulation. By varying the modeling of the track and trigger turn on curves and measuring the impact on $N_{4\mu}$ the uncertainties on track and trigger p_T thresholds have been estimated to be 9.0% and 8.4% respectively. The trigger plateau uncertainty partially cancels out in taking the $\eta \to 4\mu$ to $\eta \to 2\mu$ ratio and a residual uncertainty has been measured in data with the orthogonal trigger method. The plateau uncertainty has been conservatively estimated to be 3.2% A subdominant source of systematic uncertainty is due to the choice of fit model used to extract the signal yield in both $\eta \to 4\mu$ and $\eta \to 2\mu$ channels. This uncertainty is estimated by testing different signal and background models, resulting in a 6.6% value. Adding all the systematic uncertainties in quadrature yields an uncertainty of 14%.

8. Results

The resulting $\mathcal{B}_{4\mu}/\mathcal{B}_{2\mu}$ ratio is

$$\frac{\mathcal{B}_{4\mu}}{\mathcal{B}_{2\mu}} = [0.86 \pm 0.14(\text{stat}) \pm 0.12(\text{syst})] \times 10^{-3}\,.$$

Using the world-average value of a $\mathcal{B}(\eta \to 2\mu) = (5.8 \pm 0.8) \times 10^{-6}$ [1] the branching fraction of the η decaying to 4μ is

$$\mathcal{B}(\eta \to 4\mu) = [5.0 \pm 0.8(\text{stat}) \pm 0.7(\text{syst}) \pm 0.7(\mathcal{B}_{2\mu})] \times 10^{-9}\,,$$

a measurement which is in good agreement with the theoretical prediction of $(3.98 \pm 0.15) \times 10^{-9}$[18].

References

[1] P.D.G. et al., *Review of particle physics*, *Progress of Theoretical and Experimental Physics* **2022** (2022) 083C01 [https://academic.oup.com/ptep/article-pdf/2022/8/083C01/49175539/ptac097.pdf].

[2] L. Gan, B. Kubis, E. Passemar and S. Tulin, *Precision tests of fundamental physics with η and η' mesons*, *Physics Reports* **945** (2022) 1.

[3] CMS collaboration, *CMS luminosity measurement for the 2017 data-taking period at $\sqrt{s}$ = 13 TeV*, CMS Physics Analysis Summary CMS-PAS-LUM-17-004 (2018).

[4] CMS collaboration, *CMS luminosity measurement for the 2018 data-taking period at $\sqrt{s}$ = 13 TeV*, CMS Physics Analysis Summary CMS-PAS-LUM-18-002 (2019).

[5] CMS collaboration, *The CMS experiment at the CERN LHC*, *JINST* **3** (2008) S08004.

[6] CMS collaboration, *Development of the CMS detector for the CERN LHC Run 3*, *JINST* **19** (2024) P05064.

[7] CMS collaboration, *Performance of the CMS Level-1 trigger in proton-proton collisions at* $\sqrt{s} = 13$ *TeV*, *JINST* **15** (2020) P10017 [2006.10165].

[8] CMS collaboration, *The CMS trigger system*, *JINST* **12** (2017) P01020 [1609.02366].

[9] CMS collaboration, *Performance of the CMS high-level trigger during LHC run 2*, *JINST* **19** (2024) P11021 [2410.17038].

[10] CMS collaboration, *Electron and photon reconstruction and identification with the CMS experiment at the CERN LHC*, *JINST* **16** (2021) P05014 [2012.06888].

[11] CMS collaboration, *Performance of the CMS muon detector and muon reconstruction with proton-proton collisions at* $\sqrt{s} = 13$ *TeV*, *JINST* **13** (2018) P06015 [1804.04528].

[12] CMS collaboration, *Description and performance of track and primary-vertex reconstruction with the CMS tracker*, *JINST* **9** (2014) P10009 [1405.6569].

[13] CMS collaboration, *Particle-flow reconstruction and global event description with the CMS detector*, *JINST* **12** (2017) P10003 [1706.04965].

[14] CMS collaboration, *Performance of reconstruction and identification of* τ *leptons decaying to hadrons and* ν_τ *in pp collisions at* $\sqrt{s} = 13$ *TeV*, *JINST* **13** (2018) P10005 [1809.02816].

[15] CMS collaboration, *Jet energy scale and resolution in the CMS experiment in pp collisions at 8 TeV*, *JINST* **12** (2017) P02014 [1607.03663].

[16] CMS collaboration, *Performance of missing transverse momentum reconstruction in proton-proton collisions at* $\sqrt{s} = 13$ *TeV using the CMS detector*, *JINST* **14** (2019) P07004 [1903.06078].

[17] CMS collaboration, *Data Parking and Data Scouting at the CMS Experiment*, .

[18] R. Escribano and S. Gonzàlez-Solís, *A data-driven approach to* π^0, η *and* η' *single and double dalitz decays**, *Chinese Physics C* **42** (2018) 023109.

[19] CMS Collaboration collaboration, *Observation of the rare decay of the* η *meson to four muons*, *Phys. Rev. Lett.* **131** (2023) 091903.

[20] I. Froehlich, *Pluto: A monte carlo simulation tool for hadronic physics*, 2007.

[21] T. Sjöstrand, *An introduction to pythia 8.2*, *Computer Phys. Comm.* **191** (2015) 159.

[22] GEANT4 collaboration, *G4 - a simulation toolkit*, *Nucl. Instrum. Meth. A* **506** (2003) 250.

[23] CELSIUS/WASA Collaboration collaboration, *Measurement of* η *meson decays into lepton-antilepton pairs*, *Phys. Rev. D* **77** (2008) 032004.

[24] B. Borasoy and R. Nißler, $\eta, \eta' \to \pi l^+ l^-$ *in a chiral unitary approach*, *The European Physical Journal A* **33** (2007) 95.